[CANCER RESEARCH 59, 2411–2416, May 15, 1999]

A New *in Vivo* Method to Study P-Glycoprotein Transport in Tumors and the Blood-Brain Barrier[1]

N. Harry Hendrikse, Elisabeth G. E. de Vries,[2] Lizette Eriks-Fluks, Winette T. A. van der Graaf, Geke A. P. Hospers, Antoon T. M. Willemsen, Willem Vaalburg, and Eric J. F. Franssen

Positron Emission Tomography Center [N. H. H., L. E-F., A. T. M. W., W. V., E. J. F. F.], Department of Medical Oncology [N. H. H., E. G. E. d. V., W. T. A. v. d. G., G. A. P. H.], Groningen University Hospital, 9700 RB Groningen, the Netherlands

ABSTRACT

Drug resistance is a major cause of chemotherapy failure in cancer treatment. One reason is the overexpression of the drug efflux pump P-glycoprotein (P-gp), involved in multidrug resistance (MDR). *In vivo* pharmacokinetic analysis of P-gp transport might identify the capacity of modulation by P-gp substrate modulators, such as cyclosporin A. Therefore, P-gp function was measured *in vivo* with positron emission tomography (PET) and [^{11}C]verapamil as radiolabeled P-gp substrate.

Studies were performed in rats bearing tumors bilaterally, a P-gp-negative small cell lung carcinoma (GLC_4) and its P-gp-overexpressing subline (GLC_4/P-gp). For validation, *in vitro* and biodistribution studies with [^{11}C]daunorubicin and [^{11}C]verapamil were performed.

[^{11}C]Daunorubicin and [^{11}C]verapamil accumulation were higher in GLC_4 than in GLC_4/P-gp cells. These levels were increased after modulation with cyclosporin A in GLC_4/P-gp. Biodistribution studies showed 159% and 185% higher levels of [^{11}C]daunorubicin and [^{11}C]verapamil, respectively, in GLC_4 than in GLC_4/P-gp tumors. After cyclosporin A, [^{11}C]daunorubicin and [^{11}C]verapamil content in the GLC_4/P-gp tumor was raised to the level of GLC_4 tumors. PET measurements demonstrated a lower [^{11}C]verapamil content in GLC_4/P-gp tumors compared with GLC_4 tumors. Pretreatment with cyclosporin A increased [^{11}C]verapamil levels in GLC_4/P-gp tumors (184%) and in brains (1280%). This pharmacokinetic effect was clearly visualized with PET.

These results show the feasibility of *in vivo* P-gp function measurement under basal conditions and after modulation in solid tumors and in the brain. Therefore, PET and radiolabeled P-gp substrates may be useful as a clinical tool to select patients who might benefit from the addition of a P-gp modulator to MDR drugs.

INTRODUCTION

Resistance of tumors to chemotherapeutic drugs is a major problem in the treatment of cancer patients. Important anticancer drugs, such as anthracyclines (daunorubicin and doxorubicin), *Vinca* alkaloids (vincristine, vinblastine), epipodophyllotoxins (etoposide), and taxanes (paclitaxel) are involved in the so-called MDR[3] (1–5). Several mechanisms are responsible for MDR. One of them is the overexpression of the *MDR1* gene, resulting in increased levels of the ATP-dependent M_r 170,000 P-gp drug efflux pump (2, 6–8). Apart from the above-mentioned anticancer drugs, several other nonchemotherapeutic drugs are substrates for this pump (9–19). For instance, for several HIV-1 protease inhibitors such as indinavir, nelfinavir, and saquinavir, it is shown *in vitro* and *in vivo* that P-gp plays a role in the transport function of these HIV-1 protease inhibitors (19). Also cyclosporin A (immunosuppressive agent), domperidone (antiemetic agent), and loperamide (antidiarrheal drug) are transported by P-gp (18). To overcome MDR, several drugs have been identified that can inhibit transport by P-gp in P-gp-expressing tissues. Modulation with relatively nontoxic reversal agents such as cyclosporin A and its nonimmunosuppressive analogue PSC833 might increase the pharmacological effects of MDR involved chemotherapeutic drugs in different normal tissues (20, 21) and in P-gp-overexpressing solid tumors. However, until now, clinical studies in solid tumors combining reversal agents with MDR chemotherapeutic drugs are relatively disappointing (10, 22, 23). However, in these studies the P-gp functionality in the tumors is unknown. In these tumors P-gp may be present but does not have to be functional. Then modulation will be disappointing. A technique that would allow us to visualize blockade by modulators of the P-gp drug efflux pump might help to select the proper patients for treatment of MDR involved chemotherapeutic drugs in combination with a modulator. Until now, several studies have been described with ^{99m}Tc-labeled substrates and single photon emission computed tomography to visualize a decreased uptake of ^{99m}Tc-sestamibi and ^{99m}Tc-Q-complexes in solid tumors and in the blood-brain barrier due to P-gp expression (24–28). However, we and others observed for example that ^{99m}Tc-sestamibi is apart from P-gp, also a substrate for MRP (29, 30). In the present study, the pharmacokinetics of [^{11}C]verapamil is investigated with PET in tumor-bearing rats. For these studies, rats were inoculated with a human P-gp-negative small cell lung carcinoma cell line GLC_4 and its *MDR1* gene-transfected, P-gp-overexpressing subline GLC_4/P-gp. The potential of imaging P-gp reversal effect by cyclosporin A on the tumor pharmacokinetics of [^{11}C]verapamil was analyzed by PET and validated with biodistribution studies with [^{11}C]daunorubicin and [^{11}C]verapamil. Namely, when [^{11}C]verapamil is combined with cyclosporin A, both compounds are actively transported by P-gp. Because of competition for P-gp, the amount of transported [^{11}C]verapamil will be diminished, resulting in increased radioactivity in the tumor.

MATERIALS AND METHODS

Chemicals. RPMI 1640 and FCS were purchased from Life Technologies, Inc. (Paisley, United Kingdom) and 3-(4,5-dimethyl-thiazol-2-yl)-2,5-diphenyl tetrazolium bromide from Sigma Chemical Co. (St. Louis, MO). Ketamine (Ketalar; 50 mg/ml) was obtained from Parke-Davis (Münich, Germany), xylazine (Rompun solution 2%) was from Bayer (Leverkusen, Germany), cyclosporin A (50 mg/ml) in Cremophor EL (650 mg/ml; Sandimmune) was from Sandoz (Basel, Switzerland), Matrigel was from Becton Dickinson (Bedford, MA), and C219 was from Thamer Diagnostica (Uithoorn, the Netherlands). *N*-Nor-methyl verapamil was purchased from RBI (Natick, MA), and vincristine was from Eli Lilly (Indianapolis, IN). 9-Formyl trifluoroacetyl daunorubicin was a kind gift from Farmitalia Carlo Erba (Dr. Suarato, Milano, Italy).

Preparation of [^{11}C]Daunorubicin and [^{11}C]Verapamil. [^{11}C]D,L-daunorubicin and [^{11}C]D,L-verapamil ($t_{1/2}$ = 20.4 min) were prepared as described by Elsinga *et al.* (31). The specific activity of [^{11}C]daunorubicin was >370 GBq/mmol and [^{11}C]verapamil was 555 GBq/mmol at the end of the synthesis. The ^{11}C-labeled radiopharmaceuticals were purified by high-pres-

Received 10/22/98; accepted 3/21/99.

The costs of publication of this article were defrayed in part by the payment of page charges. This article must therefore be hereby marked *advertisement* in accordance with 18 U.S.C. Section 1734 solely to indicate this fact.

[1] This project was supported by Grant GUKC 94-783 of the Dutch Cancer Society.

[2] To whom requests for reprints should be addressed, at Division of Medical Oncology, Department of Internal Medicine, University Hospital, P. O. Box 30.001, 9700 RB Groningen, the Netherlands. Phone: 31-50-3616161; Fax: 31-50-3614862; E-mail: e.g. e.de.vries@int.azg.nl.

[3] The abbreviations used are: MDR, multidrug resistance; P-gp, P-glycoprotein; PET, positron emission tomography; IC_{50}, drug concentration inhibiting survival by 50%; MRP, multidrug resistance-associated protein; HPLC, high-performance liquid chromatography.

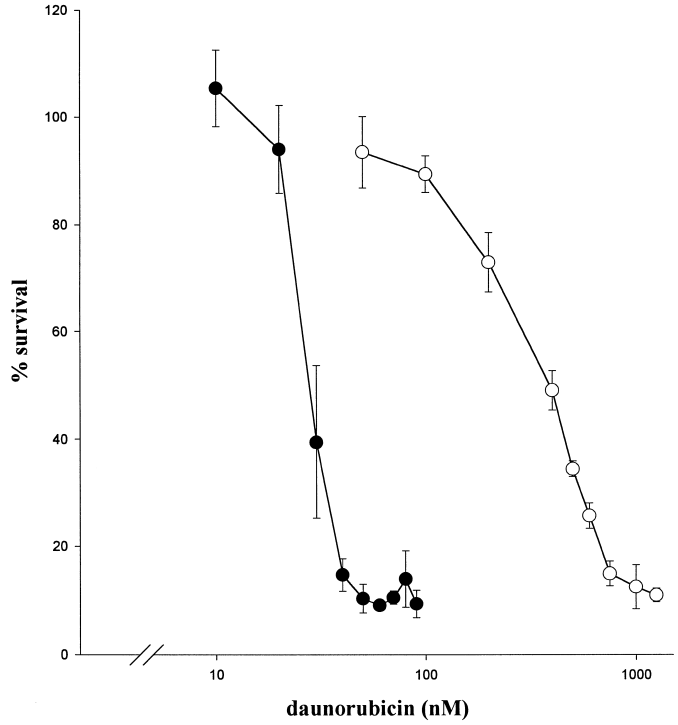

Fig. 1. Cell survival after 1 h incubation with daunorubicin in GLC_4 (●) and GLC_4/P-gp (○). At all concentrations, survival of GLC_4 was significantly reduced compared with GLC_4/P-gp. Each point represents the mean of three independent experiments, each performed in quadruplicate; *bars*, SD.

sure liquid chromatography (31). After evaporation of the eluent, radioactivity was dissolved in sterile saline.

Cells Lines. The human small cell lung carcinoma cell line GLC_4 and the human small cell lung carcinoma cell line GLC_4/P-gp were cultured in RPMI 1640/10% FCS in a humidified atmosphere with 5% CO_2 at 37°C. The P-gp-overexpressing cell line was obtained after infection of GLC_4 cells with a *MDR1* gene-carrying retrovirus. The *MDR1* gene was introduced into the retrovirus-producing packaging cell line GP+envAm12, and clones resistant to 50 nM vincristine were pooled (32). The virus titer was 1×10^4 vincristine-resistant colony-forming units/ml on NIH-3T3 cells. Subsequently, GLC_4 tumor cells were infected with virus supernatant, and selection with 50 nM vincristine resulted in the GLC_4/P-gp subline. Stable resistance in the GLC_4/P-gp cell line was assured by culturing this line in the presence of vincristine (50 nM) twice a week. Daunorubicin resistance was tested *in vitro* with a cytotoxicity test, the microculture tetrazolium assay (33). Cells in logarithmic growth phase, 3,750 and 10,000 per well for GLC_4 and GLC_4/P-gp, respectively, were incubated for 4 days with daunorubicin. For GLC_4 cells, the concentration range was 10–90 nM and 50–1250 nM in 0.1 ml of culture medium for GLC_4/P-gp. On day 4, the percentage of cell survival was calculated as the mean of test samples/mean of untreated samples. Controls consisted of media without cells (background extinction) and cells incubated with medium instead of the drug. Three independent experiments were performed, each in quadruplicate. Results were expressed as mean ± SD. From the survival curves, the daunorubicin concentrations were determined that inhibited cell survival by 50% (IC_{50}).

Animal Model. Male nude rats (HSD Ham RNU rnu; Harlan, Horst, the Netherlands; 280–300 g; age, 6 weeks) were injected with GLC_4 and GLC_4/P-gp tumor cells (10^7 cells/0.1 ml RPMI/FCS 10%). Before injection of tumor cells, GLC_4 and GLC_4/P-gp cells (10^7/0.1 ml RPMI/FCS 10%) were mixed with 0.1 ml Matrigel. Subsequently, the GLC_4 or GLC_4/P-gp cell suspension was injected s.c. in the left and the right sides, respectively, of the nude rat. Ten to 14 days after injection of the cells, solid tumor nodules of ~1 cm diameter were grown. Thereafter, the tumors were removed, and pieces of GLC_4 and GLC_4/P-gp tumors (~2–3 mm in diameter) were transplanted in the left and the right sides, respectively, in other male nude rats (HSD Ham RNU rnu; Harlan). Fourteen days after transplantation of these GLC_4 and GLC_4/P-gp tumor pieces, tumors of 1–2 cm in diameter were developed. These rats were used various experimental settings. All experiments were carried out in compliance with the local guidelines.

Tumor Histology. To allow histological data of GLC_4 and GLC_4/P-gp tumors, the 1–2 cm-sized tumors were excised and frozen in liquid nitrogen. From the frozen tumor tissue, 4-μm slices were cut. The cell viability and the cell density were measured in H&E-stained slides. Cell density was scored by counting the cells in 10 microscopic fields of 2.5×10^{-4} mm^3 ($0.25 \times 0.25 \times 0.004$ mm) microscopic fields on H&E-stained slides obtained from three different tumors for both tumor types (mean ± SD).

P-gp Expression. The P-gp expression in cell lines and tumor tissue was tested with the P-gp-directed monoclonal antibody C219. To check whether the MRP_1 expression was induced, MRP_1 was stained with monoclonal antibody MRPrl (kindly provided by Dr. R. Scheper, Free University, Amsterdam, the Netherlands) on cytospins and tumor tissue (34).

Cellular Accumulation of [^{11}C]Daunorubicin and [^{11}C]Verapamil in Tumor Cells. A total of 2×10^6 GLC_4 and GLC_4/P-gp cells were incubated in polystyrene tubes for 60 min at 37°C with 5 μM [^{11}C]daunorubicin or 5 μM [^{11}C]verapamil in 5 ml of RPMI 1640/10% FCS. To study modulating effects, GLC_4 and GLC_4/P-gp cell lines were incubated simultaneously with cyclosporin A (50 μM) and daunorubicin (5 μM) or verapamil (5 μM). Thereafter, the cells were washed with 5 ml of ice-cold PBS (0.14 M NaCl, 2.7 M KCl, 6.4 mM Na_2HPO_4, and 1.5 mM KH_2PO_4, pH 7.4), followed by centrifugation (5 min of 180 g; 4°C). The supernatant was removed, and the cellular radioactivity was measured in water in a gamma counter (LKB Wallac, Turku, Finland). Correction for the extracellular adhesion of radioactivity to polystyrene tubes was performed by subtracting the results obtained after incubation with [^{11}C]daunorubicin or [^{11}C]verapamil for 60 min at 4°C. The cellular accumulation is expressed as % dose/10^6 cells (mean ± SD).

Conventional Biodistribution of [^{11}C]Daunorubicin and [^{11}C]Verapamil in Nude Rats. Tumor rats were anesthesized with ketamine:xylazine (2:1; 1 ml/kg). Thereafter, 0.3 ml [^{11}C]daunorubicin (10 mg/kg) or [^{11}C]verapamil (0.1 mg/kg) was injected into the tail vein. After 60 min, the rats were sacrificed by extirpation of the heart, and several tissues were dissected. Heparin-plasma was obtained from the collected blood by centrifugation (3 min; 1000 g). Radioactivity was measured with a gamma counter. Modulation of [^{11}C]daunorubicin and [^{11}C]verapamil kinetics with cyclosporin A was tested in the nude rats. Cyclosporin A was injected into the penile vein (50 mg/kg). After 30 min, [^{11}C]verapamil or [^{11}C]daunorubicin was administered into the tail vein. Sixty min after the injection of [^{11}C]verapamil or [^{11}C]daunorubicin, the biodistribution of ^{11}C-labeled radioactivity was measured as described above. Results are expressed as ng/g tumor for [^{11}C]verapamil and as μg/g tumor for [^{11}C]daunorubicin.

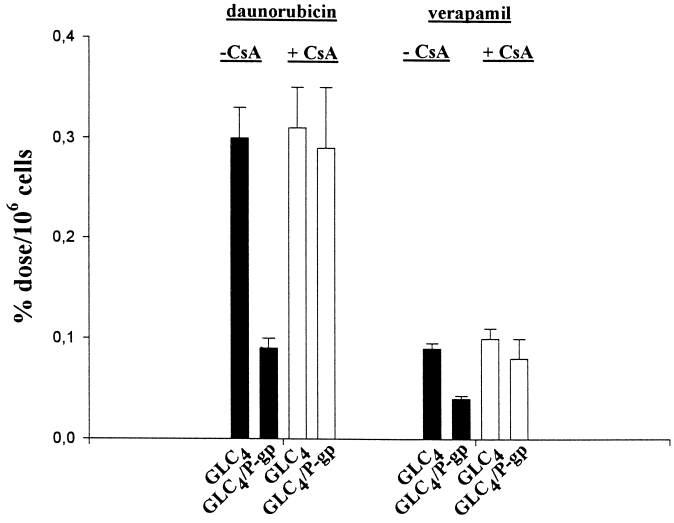

Fig. 2. [^{11}C]Daunorubicin and [^{11}C]verapamil accumulation (*y-axis*) in GLC_4 and GLC_4/P-gp tumor cells (*x-axis*) after 1 h incubation plus (○) or minus (●) 50 μM cyclosporin A. Data are expressed as means of three independent experiments, each performed in duplicate; *bars*, SD.

Radioactivity Clearance from Plasma. Rats were anesthesized as described above, and the carotid artery was cannulated. Arterial blood samples (100–200 μl) were drawn at various time points from 0–60 min after injection of the ^{11}C-labeled radioactivity. Plasma and RBCs were separated by centrifugation (3 min; 3000 g). Plasma (50 μl) samples were counted in a calibrated gamma counter. Results were expressed as mean ± SD.

Analysis of [^{11}C]Verapamil Metabolism. For analysis of [^{11}C]verapamil, 1 h after injection of radioactivity in the penile vein, the rats were sacrificed by extirpation of the heart. In the brain, the plasma and both tumors, metabolism of [^{11}C]verapamil was studied. These tissues were homogenized in acetonitrile (2 ml), using a Heidolph Diax 600 apparatus (Salm and Kipp b.v., Breukelen, the Netherlands). Thereafter, the extracts were centrifuged (3 min; 3000 g), and acetonitrile was evaporated under reduced pressure at 50°C. To the extracts of the brain and the tumors, 180 μl of sterile water, 20 μl of sodium hydroxide (0.1 M), and 1 ml of diaethyl-ether was added. The mixtures were vortexed for 1 min and centrifuged (5 min; 3000 g). The organic phase was separated and acidified with 300 μl of sulfuric acid (0.5 M). Subsequently, the mixtures were vortexed for 1 min and centrifuged (5 min; 3000 g). To the supernatant, 350 μl of sterile water was added, and this was applied onto a HPLC column [Novapack C18 4 μm, 150 × 3.9 mm; mobile phase, KH_2PO_4 (0.1 M): acetonitrile = 70:30; pH 2.5 by addition of ortho-phosphoric acid; flow rate, 1.0 ml/min]. Fractions (0.5 ml) of the eluate were collected during 10 min and counted in a calibrated gamma counter (LKB Wallac, Turku, Finland). The radioactive recovery was >80%. The recovery was calculated as follows. Before injection of radioactivity on HPLC, the radioactivity was counted in a gamma counter. After separation of fractions on a HPLC column, all of the fractions were counted, and the eluted percentage of radioactivity over the HPLC column was calculated. Results are expressed as percentage of parent compound (mean ± SD).

PET Studies in Tumor-bearing Rats. The pharmacokinetics of [^{11}C]verapamil in rats were studied with a positron camera. After anesthesia as described above, the long axis of the rat was positioned in the PET camera (ECAT 951/31 positron camera; Siemens/CTI, Knoxville, TN) parallel to the transaxial plane of the tomograph to obtain sagittal sections. A transmission scan to correct for attenuation of photons by the body tissues was obtained immediately before the emission scan. Because of homogeneous diffusion of [^{15}O]H_2O over the rat body, a PET-[^{15}O]H_2O study is useful for a good anatomical localization of the brain and the tumors. Therefore, [^{15}O]H_2O (37 MBq) dissolved in 0.3 ml of saline was injected into the tail vein. The following frames were acquired: 4 consecutive frames of 5 s, 1 frame of 10 s, 2 consecutive frames of 30 s, and 1 frame of 120 s. Twenty min after injection of [^{15}O]H_2O, [^{11}C]verapamil (37 MBq, 0.1 mg/kg) was injected into the tail vein. The following frames were acquired: 12 consecutive frames of 10 s, 6 of 30 s, 5 of 60 s, 5 of 120 s, and 8 of 300 s. After finishing [^{11}C]verapamil kinetics, cyclosporin A (50 mg/kg, i.v.) was injected into the penile vein. Thirty min after injection of cyclosporin A, [^{11}C]verapamil (0.1 mg/kg) was injected in the tail vein, and an emission scan was obtained as described above. Therefore, in this experimental setting, the rats were their own controls when modulating effects of cyclosporin A on [^{11}C]verapamil kinetics in GLC_4 and GLC_4/P-gp tumors were investigated. In addition, to avoid carryover of the first [^{11}C]verapamil injection, there was a time interval of at least 100 min between both injections. After 100 min, only ±3% of [^{11}C] radioactivity could be present when [^{11}C]verapamil was injected for the second time. Radioactive decay was corrected automatically, and data analysis was performed using the Siemens ECAT software (V6.3 D) on a Sun workstation. Results are expressed as percentage of injected dose/ml tumor.

Statistical Analysis. Differences in ^{11}C accumulation in GLC_4 and GLC_4/P-gp tumors and differences in ^{11}C accumulation with and without cyclosporin A modulation were analyzed using Wilcoxon's test (two-sided). $P < 0.05$ were considered significant.

RESULTS

Cytotoxicity Assay. Cell survival curves of the GLC_4 and GLC_4/P-gp cell lines after exposure to daunorubicin are shown in Fig. 1. GLC_4 is 12.2-fold more sensitive for daunorubicin than GLC_4/P-gp. The IC_{50}s for daunorubicin are 36 nM for GLC_4 cell line and 440 nM for the GLC_4/P-gp cell line.

Cellular Accumulation of [^{11}C]Daunorubicin and [^{11}C]Verapamil. Cellular accumulation of [^{11}C]daunorubicin and [^{11}C]verapamil were 3.3-fold ($P < 0.001$) and 2.3-fold ($P < 0.001$) higher, respectively, in GLC_4 compared with GLC_4/P-gp. Coincubation with cyclosporin A increased the cellular content of [^{11}C]daunorubicin and [^{11}C]verapamil in GLC_4/P-gp 3.2-fold ($P < 0.005$) and 2.0-fold ($P < 0.02$), respectively. Cyclosporin A did not affect the cellular content of [^{11}C]daunorubicin and [^{11}C]verapamil in GLC_4 cells (Fig. 2). In addition, although the ratio of [^{11}C]daunorubicin accumulation in GLC_4 and GLC_4/P-gp is higher than the [^{11}C]verapamil ratio, only camera studies *in vivo* with [^{11}C]verapamil were performed. The reason for this was the fact that [^{11}C]verapamil production could be scaled up so that sufficiently high enough radioactivity allowed extensive *in vivo* studies in rats using the positron camera.

Tumor Histology. A semiquantitative assessment demonstrated that >80–90% of the cells in both tumor types were viable. The GLC_4 and the GLC_4/P-gp tumors consisted of tumor cells, blood vessels, and rat stroma. Histology revealed that in GLC_4 tumors, the cell density was lower than in GLC_4/P-gp tumors ($P = 0.0008$; $n = 3$). The cell density in GLC_4 tumors was $8.7 \times 10^9 \pm 0.7 \times 10^9$ cells/ml tumor and in GLC_4/P-gp tumors, $13 \times 10^9 \pm 0.4 \times 10^9$ cells/ml tumor. GLC_4 tumor tissue showed no P-gp expression, and GLC_4/P-gp stained clearly for P-gp. Furthermore, the GLC_4 and GLC_4/P-gp tumors showed an equally weak MRP_1 staining (data not shown).

Conventional Biodistribution of [^{11}C]Daunorubicin and [^{11}C]Verapamil in Tumor Tissue of Tumor-bearing Nude Rats. One h after injection, the [^{11}C]daunorubicin content was 159 ± 28% higher ($n = 4$; $P < 0.05$) in GLC_4 tumors than in GLC_4/P-gp tumors. Results for individual animals with their paired tumors are shown in Fig. 3*A*. Modulation with cyclosporin A (50 mg/kg) increased the [^{11}C]daunorubicin levels in the GLC_4/P-gp tumor to the same levels as compared with GLC_4 tumors (Fig. 3*B*). In addition, after modulation with cyclosporin A, [^{11}C]daunorubicin levels were not significantly increased in any other tissue than the GLC_4/P-gp tumor (data not shown). After injection of [^{11}C]verapamil, the verapamil content was 184 ± 53% higher ($n = 5$; $P < 0.05$) in GLC_4 tumors than in GLC_4/P-gp tumors (Fig. 4*A*).The tissue levels obtained after injection of [^{11}C]verapamil are summarized in Table 1. After modulation with cyclosporin A (50 mg/kg), the [^{11}C]verapamil content in the GLC_4/P-gp tumor was raised to the level of the GLC_4 tumor (Fig. 4*B*). In addition, the results of the [^{11}C]verapamil content observed in other tissues are shown in Table 1. One h after injection of [^{11}C]verapamil, [^{11}C]verapamil was present as parent compound for 90 ± 7% ($n = 3$) in GLC_4 and GLC_4/P-gp tumor tissue, in plasma for 83 ± 5% ($n = 5$), and in the brain for 93 ± 5% ($n = 3$).

Plasma Clearance in Tumor-bearing Nude Rats. Plasma clearance of ^{11}C was rapid after [^{11}C]daunorubicin injection (10 mg/kg; data not shown). The curve showed a biphasic pattern. The first phase had a half-life of 0.70 min, and the second phase had a half-life of 69.3 min. After [^{11}C]verapamil injection (0.1 mg/kg), a biphasic plasma curve was shown (data not shown). The first phase had a half-life of 0.50 min, and the second phase had a half-life of 69.3 min. Furthermore, no significant differences in [^{11}C]daunorubicin and [^{11}C]verapamil arterial plasma kinetics were observed after modulation with cyclosporin A (data not shown).

PET of [^{15}O]H_2O in the Brain and the Tumors of the Rat. Experiments were performed with [^{15}O]H_2O). PET-H_2O images enable separate localization of the tumor and the head region (data not shown).

PET of [^{11}C]Verapamil in the Brain and the Tumors of the Rat. Time activity curves after [^{11}C]verapamil injection (0.1 mg/kg) were obtained from PET images (Fig. 5) in three different rats. Fig. 6*A* demonstrates different pharmacokinetics in GLC_4 and GLC_4/P-gp

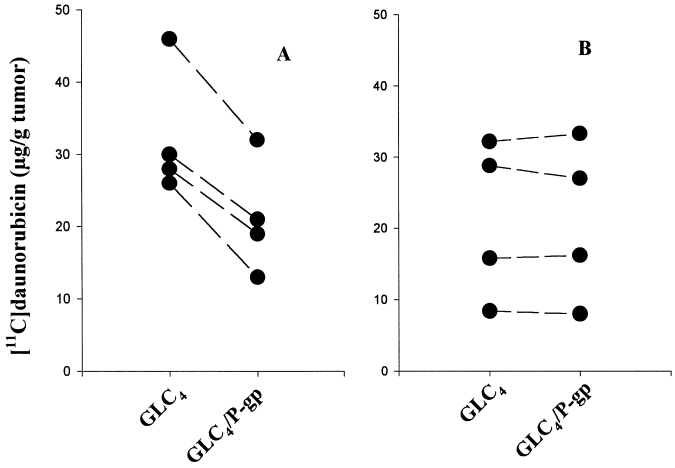

Fig. 3. Radioactivity content in GLC_4 and GLC_4/P-gp tumors 1 h after exposure to [^{11}C]daunorubicin (10 mg/kg) in the absence (*A*) and presence (*B*) of cyclosporin A (50 mg/kg). The content was expressed as μg [^{11}C]daunorubicin/g tumor. Each paired set of points represents the radioactivity level in rat-bearing tumors bilaterally. In each animal, the [^{11}C]daunorubicin content was significantly increased in GLC_4 tumors compared with GLC_4/P-gp tumors ($P < 0.05$). After modulation with cyclosporin A, there was no significant difference between [^{11}C]daunorubicin levels in GLC_4 tumors and GLC_4/P-gp tumors.

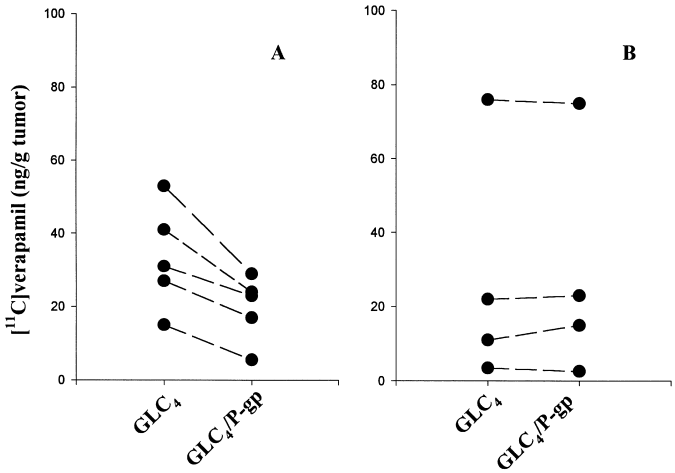

Fig. 4. Radioactivity content in GLC_4 and GLC_4/P-gp tumors 1 h after exposure to [^{11}C]verapamil (0.1 mg/kg) in the absence (*A*) and presence (*B*) of cyclosporin A (50 mg/kg). The content was expressed as ng [^{11}C]verapamil/g tumor. Each paired set of points represents the radioactivity level in a two-sided tumor-bearing rat. In each animal, the [^{11}C]verapamil content significantly increased in GLC_4 tumors compared with GLC_4/P-gp tumors ($P < 0.05$). After modulation with cyclosporin A, there was no significant difference between [^{11}C]verapamil levels in GLC_4 tumors and GLC_4/P-gp tumors.

tumors. In both tumor types, the maximum radioactivity per tumor volume was reached within 5 min after injection of the radioactivity. In the GLC_4/P-gp tumor, the maximum was 23% lower than in GLC_4 tumor 5 min after injection of [^{11}C]verapamil. After pretreatment with cyclosporin A (50 mg/kg), the accumulation of [^{11}C]verapamil was increased to an equal level as in the GLC_4 tumor (Fig. 6*B*). In the rat brain, 20 min after injection of [^{11}C]verapamil, the accumulation was 350% higher in the presence of cyclosporin A (50 mg/kg) than without cyclosporin A (Fig. 7). This result demonstrates visualization of a P-gp blockade by [^{11}C]verapamil-PET in the GLC_4/P-gp tumor and the brain after modulation with cyclosporin A.

DISCUSSION

The present study demonstrates that PET enables the measurement of P-gp mediated pharmacokinetics of [^{11}C]verapamil in solid tumors and in the blood-brain barrier. To study these kinetics, a rat model was developed. As tumor model, both a *MDR1* gene-transfected, P-gp-overexpressing human small cell lung carcinoma GLC_4/P-gp and its P-gp negative small cell lung carcinoma counterpart GLC_4 were used. Because in each rat both a P-gp-negative and a P-gp-positive tumor were xenographed, equal systemic pharmacokinetics were guaranteed. For validation of the cell lines, *in vitro* studies were performed. In these studies, it was shown that in the GLC_4 cell line the accumulation of [^{11}C]daunorubicin and of [^{11}C]verapamil was increased compared with the GLC_4/P-gp cell line. Preincubation with cyclosporin A increased [^{11}C]daunorubicin and [^{11}C]verapamil levels in GLC_4/P-gp but not in GLC_4. Furthermore, in the cytotoxicity assay, the GLC_4/P-gp line was found to be 12-fold cross-resistant for daunorubicin compared with GLC_4. These results demonstrated that GLC_4 and GLC_4/P-gp cell lines were an elegant model to study P-gp functionality in the tumor-bearing rat model. Biodistribution studies demonstrated that in the P-gp-overexpressing GLC_4/P-gp tumors, the levels of [^{11}C]daunorubicin and [^{11}C]verapamil were lower than in GLC_4 tumors. Pretreatment with cyclosporin A increased the levels of [^{11}C]daunorubicin and [^{11}C]verapamil in GLC_4/P-gp tumors to the level in the GLC_4 tumors. The effects of cyclosporin A in the GLC_4/P-gp tumors were most likely due to blockade of the P-gp drug efflux by cyclosporin A. This is underscored by the fact that cyclosporin A had no effect on plasma kinetics of [^{11}C]daunorubicin and [^{11}C]verapamil in the rat.

In the blood-brain barrier, P-gp is abundantly expressed (35), and because in this study [^{11}C]verapamil levels were increased after pretreatment with cyclosporin A, we were able to show P-gp function and its reversal effects *ex vivo* and *in vivo*. This important role of P-gp in the blood-brain barrier was also shown earlier in the mouse model. In biodistribution studies in the brain of *mdr1a*(−/−) P-gp knock-out mice, drug levels of several drugs, such as verapamil, digoxin, and cyclosporin A, were found to be increased compared with *mdr1a*(+/+) wild-type mice (16, 17). Furthermore, in wild-type mice, the brain levels of digoxin were increased after blockade of P-gp in the blood-brain barrier by PSC 833 (20). The [^{11}C]daunorubicin and [^{11}C]verapamil biodistribution data are in agreement with results obtained with the radiolabeled P-gp substrate colchicine, confirming that it is possible to distinguish P-gp-expressing tumors from sensitive tumors *in vivo* by ^{11}C-radiolabeled drugs (36–38). In contrast to verapamil, the daunorubicin levels in the brain were not increased after modulation with cyclosporin A. Daunorubicin is a substrate for P-gp as well as MRP_1. Because of expression of MRP_1 in many tissues in the body, including the blood-brain barrier (39), it might be

Table 1 *Tissue levels of radioactivity in tumor-bearing nude rats 1 h after i.v. injection of [^{11}C]verapamil (0.1 mg/kg) (A) and effects on [^{11}C]verapamil content after modulation with cyclosporin A (50 mg/kg) (B)*

Results are expressed as mean ± SD in ng/g tissue.

Tissue	A (n = 3–5)	B (n = 3–4)	Ratio	P
Brain	7 ± 0.2	90 ± 3	12.8	0.0018
Testes	17 ± 2	23 ± 11	1.4	NS[a]
Liver	238 ± 63	216 ± 42	0.9	NS
Kidney	160 ± 64	145 ± 47	0.9	NS
Spleen	156 ± 7	175 ± 118	1.1	NS
Pancreas	119 ± 17	122 ± 29	1.0	NS
Bladder	65 ± 33	41 ± 32	0.6	NS
Heart	61 ± 18	71 ± 22	1.2	NS
Epididymis	32 ± 9	33 ± 22	1.0	NS
Small intestine	157 ± 32	185 ± 25	1.2	NS
Colon	81 ± 31	62 ± 13	0.8	NS
Lung	599 ± 320	399 ± 334	0.7	NS
Red blood cells	13 ± 4	11 ± 4	0.8	NS
GLC_4	33 ± 14	28 ± 33	1.2	NS
GLC_4/P-gp	20 ± 9	29 ± 32	0.7	NS
Plasma	30 ± 15	16 ± 6	0.5	NS

[a] NS, not significant.

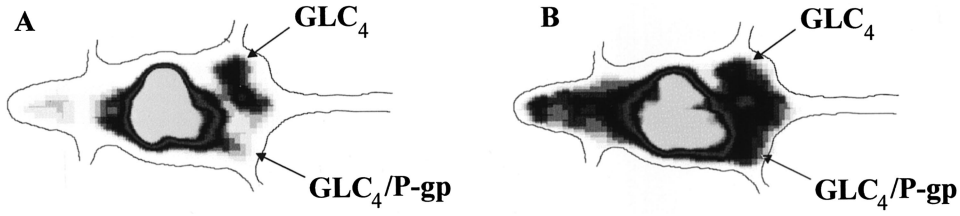

Fig. 5. A representative PET study in a male rat bearing tumors bilaterally. The images show the distribution of radioactivity after injection of [^{11}C]verapamil (0.1 mg/kg; *A*) and after injection of [^{11}C]verapamil (0.1 mg/kg) in the presence of cyclosporin A (50 mg/kg; *B*).

possible that after modulation with cyclosporin A, daunorubicin is still transported by the MRP_1 drug efflux pump.

Ex vivo data demonstrated the usefulness of P-gp-mediated [^{11}C]verapamil kinetics in the P-gp-expressing tumor and in the central nervous system. For [^{11}C]verapamil production, it was possible to scale up so that sufficiently high enough radioactivity was available for *in vivo* studies in rats and potentially for humans with a positron camera. Therefore, *in vivo* studies were performed with [^{11}C]verapamil. After injection of [^{11}C]verapamil in the rat, a fast radioactivity transport was observed in the P-gp-overexpressing tumor, and 10 min after injection, a steady-state level was reached (Fig. 6). Possibly, due to the high lipophilicity, verapamil may be bound in the tumor, preventing transport from the tumor back into the blood. Furthermore, it might be possible that other routes such as passive efflux may play an important role in the cellular transport of verapamil. It is speculated that the time-activity curve of [^{11}C]verapamil

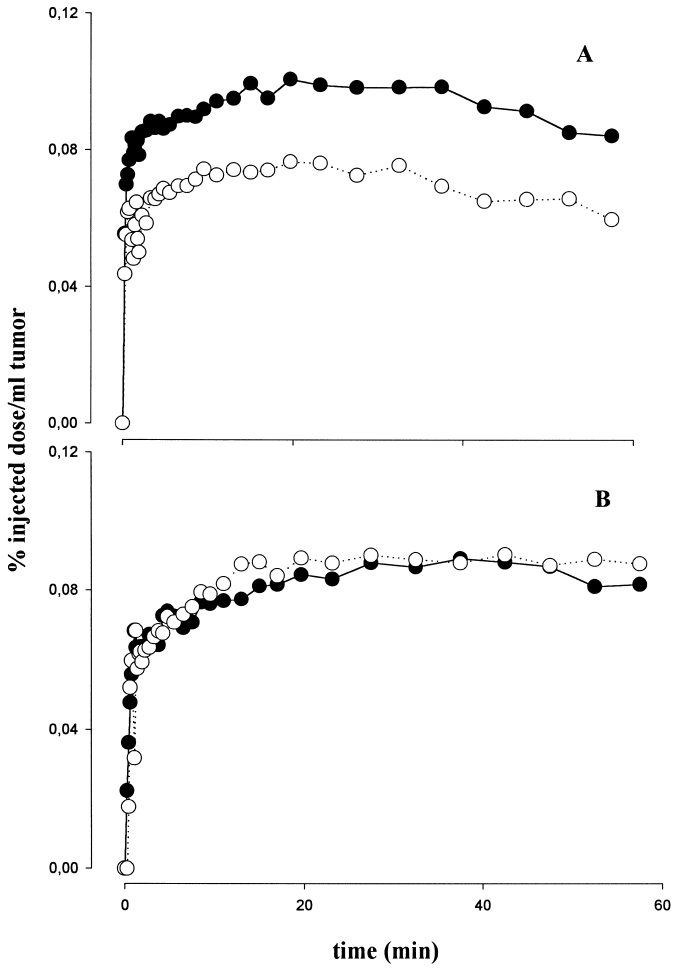

Fig. 6. A representative study demonstrating time-activity curves of [^{11}C]verapamil (0.1 mg/kg) in the absence (*A*) and presence (*B*) of cyclosporin A (50 mg/kg) in the GLC_4 (●) and the GLC_4/P-gp (○) tumor obtained from PET images.

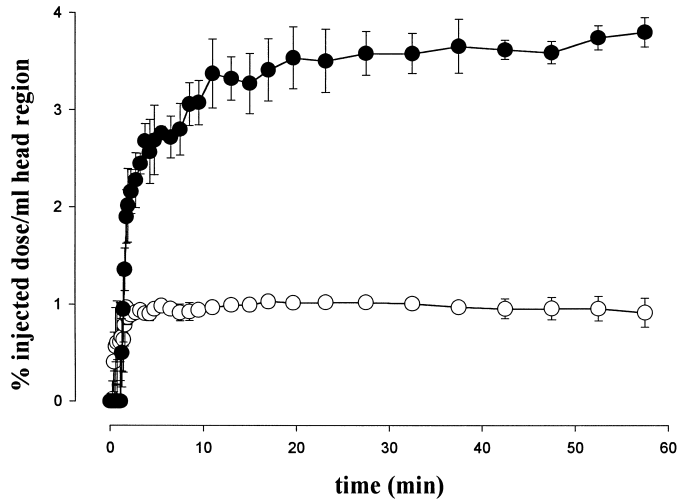

Fig. 7. Time-activity curves of [^{11}C]verapamil (0.1 mg/kg) in the absence (○) and presence (●) of cyclosporin A (50 mg/kg) in the head region of rats obtained from PET images. Each point represents the mean of three independent experiments; *bars*, SD.

might be the result of partly passive efflux of verapamil over tumor membranes and partly by P-gp-mediated pharmacokinetics. This is supported by the observed rapid cellular verapamil passive diffusion of 50% within 5 min for P-gp-negative and P-gp-positive ovarian carcinoma cell lines (40, 41).

Several experiments with ^{99m}Tc-sestamibi and other ^{99m}Tc-labeled substrates, such as ^{99m}Tc-Q-complexes and ^{99m}Tc-tetrofosmin, demonstrated in rats and in patients an increased efflux of ^{99m}Tc-sestamibi in P-gp-expressing tumor cells and modulation effects with reversal agents (24–28, 42–44). However, with single photon emission computed tomography, quantitative information about pharmacokinetics in the tumor is less accurate than with PET. Recently, we have shown that ^{99m}Tc-sestamibi is also a substrate for MRP_1 (29, 30). In contrast to ^{99m}Tc-sestamibi, [^{11}C]verapamil is a relatively poor substrate for MRP_1. This makes [^{11}C]verapamil a more specific tracer for P-gp function than ^{99m}Tc-sestamibi. Comparison of sensitivity between ^{99m}Tc-sestamibi and [^{11}C]verapamil demonstrates that ^{99m}Tc-sestamibi has the ability to image P-gp in a tumor that is 2–3-fold more resistant for doxorubicin compared with the P-gp-negative tumor (25). In contrast, [^{11}C]verapamil showed 2-fold less radioactivity in a P-gp-expressing tumor, which is 12-fold resistant for doxorubicin compared with a P-gp-negative tumor. Because of high lipophilicity of [^{11}C]verapamil, this compound most likely binds aspecificly to cellular membranes. Additional studies in cancer patients have to be performed to elucidate whether it is possible to measure low resistance factors with this PET approach in human tumors.

In conclusion, P-gp kinetics and its reversal can be visualized *in vivo* with a positron camera. This can be a new clinical tool to study the P-gp function noninvasively and to predict the effect of modulators on treatment with MDR involved chemotherapeutic drugs.

REFERENCES

1. Endicott, J. A., and Ling, V. The biochemistry of P-glycoprotein-mediated multidrug resistance. Annu. Rev. Biochem., *58:* 137–171, 1989.
2. Gottesman, M. M., and Pastan, I. Biochemistry of multidrug resistance mediated by the multidrug transporter. Annu. Rev. Biochem., *62:* 385–427, 1993.
3. Zamora, J. M., Pearce, H. L., and Beck, W. T. Physical-chemical properties shared by compounds that modulate multidrug resistance in human leukemic cells. Mol. Pharmacol., *33:* 454–462, 1988.
4. Klopman, G., Srivastava, S., Kolossvary, I., Epand, R. F., Ahmed, N., and Epand, R. M. Structure-activity study and design of multidrug-resistant reversal compounds by a computer automated structure evaluation methodology. Cancer Res., *52:* 4121–4129, 1992.
5. Selassie, C. D., Hansch, C., and Khwaja, T. A. Structure-activity relationships of antineoplastic agents in multidrug resistance. J. Med. Chem., *33:* 1914–1919, 1990.
6. Germann, U. A., Pastan, I., and Gottesman, M. M. P-glycoproteins: mediators of multidrug resistance. Semin. Cell. Biol., *4:* 63–76, 1993.
7. Doige, C. A., and Ames, G. F. ATP-dependent transport systems in bacteria and humans: relevance to cystic fibrosis and multidrug resistance. Annu. Rev. Microbiol., *47:* 291–319, 1993.
8. Schinkel, A. H., and Borst, P. Multidrug resistance mediated by P-glycoproteins. Semin. Cancer Biol., *2:* 213–226, 1991.
9. Sonneveld, P., Schoester, M., and de Leeuw, K. Clinical modulation of multidrug resistance in multiple myeloma: effect of cyclosporine on resistant tumor cells. J. Clin. Oncol., *12:* 1584–1591, 1994.
10. Sonneveld, P., Durie, B. G., Lokhorst, H. M., Marie, J. P., Solbu, G., Suciu, S., Zittoun, R., Lowenberg, B., and Nooter, K. Modulation of multidrug-resistant multiple myeloma by cyclosporin. Lancet, *340:* 255–259, 1992.
11. Grunicke, H., and Hofmann, J. Cytotoxic and cytostatic effects of antitumor agents induced at the plasma membrane level. Pharmacol. Ther., *55:* 1–30, 1992.
12. Brunton, V. G., and Workman, P. Cell-signaling targets for antitumour drug development. Cancer Chemother. Pharmacol., *32:* 1–19, 1993.
13. Wilson, W. H., Bates, S. E., Fojo, A., Bryant, G., Zhan, Z., Regis, J., Wittes, R. E., Jaffe, E. S., Steinber, S. M., Herdt, J., and Chabner, B. A. Controlled trial of dexverapamil, a modulator of multidrug resistance, in lymphomas refractory to EPOCH chemotherapy. J. Clin. Oncol., *13:* 1995–2004, 1995.
14. Wilson, W. H., Jamis-Dow, C., Bryant, G., Balis, F. M., Klecker, R. W., Bates, S. E., Chabner, B. A., Steinberg, S. M., Kohler, D. R., and Wittes, R. E. Phase I and pharmacokinetic study of the multidrug resistance modulator dexverapamil with EPOCH chemotherapy. J. Clin. Oncol., *13:* 1985–1994, 1995.
15. Abe, T., Koike, K., Ohga, T., Kubo, T., Wada, M., Kohno, K., Morie, T., Hidaka, K., and Kuwano, M. Chemosensitisation of spontaneous multidrug resistance by a 1,4-dihydropyridine analogue and verapamil in human glioma cell lines overexpressing MRP or MDR1. Br. J. Cancer, *72:* 418–423, 1995.
16. Schinkel, A. H., Wagenaar, E., Van Deemter, L., Mol, C. A. A. M., and Borst, P. Presence of the mdr1a P-glycoprotein in mice affects tissue distribution and pharmacokinetics of dexamethasone, digoxin, and cyclosporin A. J. Clin. Invest., *96:* 1698–1705, 1995.
17. Hendrikse, N. H., Schinkel, A. H., De Vries, E. G. E., Fluks, E., Van der Graaf, W. T. A., Vaalburg, W., and Franssen, E. J. F. Complete *in vivo* reversal of P-glycoprotein pump function in the blood-brain barrier visualized with positron emission tomography. Br. J. Pharmacol., *124:* 1413–1418, 1998.
18. Schinkel, A. H., Wagenaar, E., Mol, C. A. A. M., and Van Deemter, L. P-glycoprotein in the blood-brain barrier of mice influences the brain penetration and pharmacological activity of many drugs. J. Clin. Invest., *97:* 2517–2524, 1995.
19. Kim, R. B., Fromm, M. F., Wandel, C., Leake, B., Wood, A. J. J., and Roden, D. M. The drug transporter P-glycoprotein limits oral absorption and brain entry of HIV-1 protease inhibitors. J. Clin. Invest., *110:* 289–294, 1998.
20. Mayer, U., Wagenaar, E., Dorobek, B., Beijnen, J. H., Borst, P., and Schinkel, A. H. Full blockade of intestinal P-glycoprotein and extensive inhibition of blood-brain barrier P-glycoprotein by oral treatment of mice with PSC833. J. Clin. Invest., *100:* 2430–2436, 1997.
21. Hughes, C. S., Vaden, S. L., Manaugh, C. A., Price, G. S., and Hudson, L. C. Modulation of doxorubicin concentration by cyclosporin A in brain and testicular barrier tissues expressing P-glycoprotein in rats. J. Neuro-Oncol., *37:* 45–54, 1998.
22. Van der Graaf, W. T. A., Buter, J., De Vries, E. G. E., Willemse, P. H. B., Sleijfer, D. T., and Mulder, N. H. High dose oral amiodarone added to doxorubicin and vindesine for overcoming multidrug resistance in solid tumors. Annu. Oncol., *5:* 659–663, 1994.
23. Bates, S. E., Meadows, B., Goldspiel, B. R., Denicoff, A., Le, T. B., Tucker, E., Steinber, S. M., and Elwood, L. J. A pilot study of amiodarone with infusional doxorubicin or vinblastine in refractory breast cancer. Cancer Chemother. Pharmacol., *35:* 457–463, 1995.
24. Barbaris, E., Kronauge, J. F., Cohen, D., Davison, A., Jones, A. G., and Croop, J. M. Characterization of P-glycoprotein transport and inhibition *in vivo*. Cancer Res., *58:* 276–282, 1998.
25. Piwnica-Worms, D., Chiu, M. L., Budding, M., Kronauge, J. F., Kramer, R. A., and Croop, J. M. Functional imaging of multidrug-resistant P-glycoprotein with an organotechnetium complex. Cancer Res., *53:* 977–984, 1993.
26. Crankshaw, C. L., Marmion, M., Luker, G. D., Rao, V., Dahlheimer, J., Burleigh, D., Webb, E., Deutsch, K. F., and Piwnica-Worms, D. Novel technetium (III)-Q complexes for functional imaging of multidrug resistance (MDR1) P-glycoprotein. J. Nucl. Med., *39:* 77–86, 1998.
27. Luker, G. D., Rao, V. V., Crankshew, C. L., Dahlheimer, J., and Piwnica-Worms, D. Characterization of phosphine complexes of technetium (III) as transport substrates of the multidrug resistance P-glycoprotein and functional markers of P-glycoprotein at the blood-brain barrier. Biochemistry, *36:* 14218–14227, 1997.
28. Ballinger, J. R., Bannerman, J., Boxen, I., Firby, P., Hartman, N. G., and Moore, M. J. ^{99m}Technetium-tetrofosmin as a substrate for P-glycoprotein: *in vitro* studies in multidrug-resistant breast tumor cells. J. Nucl. Med., *37:* 1578–1582, 1996.
29. Hendrikse, N. H., Franssen, E. J. F., Van der Graaf, W. T. A., Meijer, C., Piers, D. A., Vaalburg, W, and De Vries, E. G. E. ^{99m}Tc-sestamibi is a substrate for P-glycoprotein and the multidrug resistance associated protein. Br. J. Cancer, *77:* 353–358, 1998.
30. Vergote, J., Moretti, J. L., De Vries, E. G. E., and Garnier-Suillerot, A. Comparison of the kinetics of active efflux of ^{99m}Tc-MIBI in cells with P-glycoprotein-mediated and multidrug-resistance protein-associated multidrug-resistance phenotypes. Eur. J. Biochem, *252:* 140–146, 1998.
31. Elsinga, P. H., Franssen, E. J. F., Hendrikse, N. H., Fluks, L., Weemaes, A. M. A., van der Graaf, W. T. A., De Vries, E. G. E., Visser, G. M., and Vaalburg, W. [^{11}C]-Labeled daunorubicin and verapamil for probing P-glycoprotein in tumors with PET. J. Nucl. Med., *37:* 1571–1575, 1996.
32. Boesen, J. J. B., Nooter, K., and Valerio, D. Circumvention of chemotherapy-induced myelosuppression by transfer of the *MDR1* gene. Biotherapy, *6:* 291–302, 1994.
33. Timmer-Bosscha, H., Hospers, G. A. P., Meijer, C., Mulder, N. H., Muskiet, F. A., Martini, I. A., Uges, D. A., and De Vries, E. G. E. Influence of docosahexaenoic acid on cisplatin resistance in a human small cell lung carcinoma cell line. J. Natl. Cancer Inst., *81:* 1069–1075, 1989.
34. Flens, M. J., Izquierdo, M. A., Scheffer, G. L., Fritz, J. M., Meijer, C. J., Scheper, R. J., and Zaman, G. J. R. Immunohistochemical detection of the multidrug resistance-associated protein MRP in human multidrug-resistant tumor cells by monoclonal antibodies. Cancer Res., *54:* 4557–4563, 1994.
35. Schinkel, A. H., Smit, J. J. M., van Tellingen, O., Beijnen, J. H., Wagenaar, E., van Deemter, L., Mol, C. A. A. M., Van der Valk, M. A., Robanus-Maandag, E. C., Te Riele, H. P. J., Berns, A. M. J., and Borst, P. Disruption of the mouse *mdr1a* P-glycoprotein gene leads to a deficiency in the blood-brain barrier and to increased sensitivity to drugs. Cell, *77:* 491–502, 1994.
36. Metha, B. M., Rosa, E., Fissekis, J. D., Bading, J. R., Biedler, J. L., and Larson, S. M. *In vivo* identification of tumor multidrug resistance with ^{3}H-colchicine. J. Nucl. Med., *33:* 1373–1377, 1992.
37. Metha, B. M., Rosa, E., Biedler, J. L., and Larson, S. M. *In vivo* uptake of [^{14}C]-colchicine for identification of tumor multidrug resistance. J. Nucl. Med., *35:* 1179–1184, 1994.
38. Metha, B. M., Levchenko, A., Rosa, E., Kim, S. W., Winnick, S., Zhang, J. J., Kalaigian, H., and Larson, S. M. Evaluation of [^{14}C]-colchicine biodistribution with whole-body quantitative autoradiography in colchicine-sensitive and -resistant xenografts. J. Nucl. Med., *37:* 312–314, 1996.
39. Kool, M., de Haas, M., Scheffer, G. L., Scheper, R. J., van Eijk, M. J. T., Juijn, J. A., Baas, F., and Borst, P. Analysis of expression of cMOAT (MRP2), MRP3, MRP4, and MRP5, homologues of the multidrug resistance-associated protein gene (MRP_1), in human cancer cell lines. Cancer Res., *57:* 3537–3547, 1997.
40. Lankelma, J., Spoelstra, E. C., Dekker, H., and Broxterman, H. J. Evidence for daunomycin efflux from multidrug-resistant 2780AD human ovarian carcinoma cells against a concentration gradient. Biochim. Biophys. Acta, *1055:* 217–222, 1990.
41. Spoelstra, E. C., Westerhoff, H. V., Dekker, H., and Lankelma, J. Kinetics of daunorubicin transport by P-glycoprotein of intact cancer cells. Eur. J. Biochem., *207:* 567–579, 1992.
42. Ballinger, J., Hua, H., Bery, B., Firby, P., and Boxen, I. ^{99m}Tc-sestamibi as an agent for imaging P-glycoprotein-mediated multi-drug resistance: *in vitro* and *in vivo* studies in a rat breast tumour cell line and its doxorubicin-resistant variant. Nucl. Med. Commun., *16:* 253–257, 1995.
43. Luker, G. D., Fracasso, P. M., Dobkin, J., and Piwnica-Worms, D. Modulation of the multidrug resistance P-glycoprotein: detection with ^{99m}Tc-Sestamibi *in vivo*. J. Nucl. Med., *38:* 369–372, 1997.
44. Del Vecchio, S., Ciarmiello, A., Pace, L., Potena, M. I., Carriero, M. V., Mainolfi, C., Thomas, R., D'Auito, G., Tsuruo, T., and Salvatore, M. Fractional retention of ^{99m}technetium-sestamibi as an index of P-glycoprotein expression in untreated breast cancer patients. J. Nucl. Med., *38:* 1348–1351, 1997.